Study of vegetation evolution in Sicily using time series analysis of remote sensing and climatic data

ENRICO BONO, FULVIO CAPODICI, GIUSEPPE CIRAOLO, GOFFREDO LA LOGGIA, ANTONINO MALTESE & LEONARDO V. NOTO

Department of Hydraulic Engineering and Environmental Applications, Università di Palermo, Viale delle Scienze 90128, Palermo, Italy

giuseppe@idra.unipa.it

Abstract During last 10 years, several studies confirmed that drought phenomena are affecting southern Mediterranean areas. One of the effects of a persistent drought is a modification of the vegetation cover and biomass. The aim of our research is to investigate and monitor the evolution of this phenomenon in Sicily using remote sensing techniques. To do this, a data set of NOAA-AVHRR multispectral images, acquired monthly from 1988 to 2005, has been calibrated and processed. A time series analysis (TSA) has been applied both on the NDVI and precipitation data sets in order to study the main characteristics of vegetation distribution during the period under investigation and to compare the vegetation evolution as a consequence of the mean monthly rainfall distribution. Results confirm the existence of a correlation (with a time lag) between rainfall oscillations and the vegetation response in terms of NDVI.

Key words correlation analysis; NDVI fluctuations; rainfall; time series analysis

INTRODUCTION

Sicily, like most zones of the southern Mediterranean area, is subject to a risk of desertification (Kosmas *et al*., 1999; Geeson *et al*., 2002). The use of satellite images can provide an essential contribution to research on the degradation of vegetation, allowing vegetation indices to be quickly determined for large areas and at moderate spatial resolution. Indices such the Normalised Difference Vegetation Index (NDVI) are usually used to describe the vegetation amount. This index is defined by the difference between the reflectance of the near infrared (NIR) and red bands normalized by their sum (Rouse *et al.*, 1974) using the following equation:

$$\mathrm{NDVI} = \frac{\mathrm{NIR} - \mathrm{Red}}{\mathrm{NIR} + \mathrm{Red}} = \frac{\rho_2 - \rho_1}{\rho_2 + \rho_1} \qquad (1)$$

where, for the case of NOAA-AVHRR (Advanced Very High Resolution Radiometer) sensors, ρ refers to the reflectance values of second and first channel.

Vegetation dynamics are strongly dependent on variations of climatic conditions. Some authors have applied the principal component analysis (PCA) to characterize the annual and interannual variability of vegetation types and its connection with the ENSO (El Ninõ Southern Oscillation) phenomena (Gurgel & Ferreira, 2003).

Some studies have confirmed this correlation (Saugier, 1996; Richard & Poccard, 1998), pointing out a time lag between the response of vegetation and climatic variations. It is very difficult to determine the length of this delay, since it depends on the type of climate, soil (Nicholson & Farrar, 1994) and vegetation. For example, Aber *et al*. (2002) found that in a forest environment in Kansas (USA) the time lag between climatic changes and vegetation response was between one and two years. Woldu Tamrat (1997) found that vegetation responds well to the total precipitation for the preceding two months in semiarid environments, while other research reports that the lag period is variable (Richard & Poccard, 1998). Other authors have found a strong relationship between vegetation response and rainfall at continental and global scale (Zhang *et al.*, 2005). Martiny *et al.* (2006) found significant correlation between rainfall and NDVI regimes in several regions of Africa.

Recently, Cuomo *et al.* (2001) have published a study on NDVI fluctuations in the southern part of Italy showing a clear reduction in vegetation activity in the period 1985–1999. In order to describe vegetation dynamics, other authors found that the use of precipitation alone is insufficient, and have therefore added other parameters such as temperature to the analysis (Schultz & Halpert, 1993; Potter & Brooks, 1998; Wang *et al.*, 2001).

The purpose of this research is to develop a better understanding of the correlation between rainfall and vegetation evolution in Sicily (south of Italy) during a study period of 12 years.

THE STUDY AREA

The study area is Sicily island as a whole (Fig. 1), characterized by particular climatic conditions influenced by its orographic nature and by the presence of the sea.

The island has a typical Mediterranean climate along the coast up to 500–600 m above sea level, and is characterized by moderate rainfall during the autumn–winter period and by scarce precipitation during the summer. Above these elevations and up

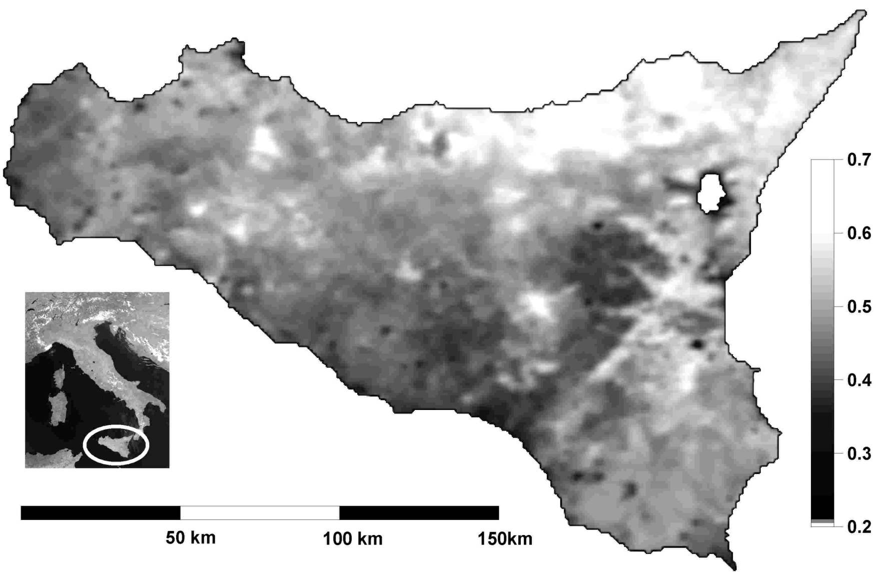

Fig. 1 Mean NDVI spatial distribution in Sicily during the period 1988–2005.

to 1200 m there is a temperate–cold climate, with mild dry summers, while a colder and rainier climate is found at higher elevations. There are two climatic seasons in Sicily; a rainy season from October to March, with maximum rainfall from November to January, and a dry period from April to September (driest from June to August).

The mean NDVI spatial distribution, displayed in Fig. 1, gives an idea of mean vegetation density spatial distribution in Sicily: the northeastern zone (Nebrodi and Madonie mountains) is covered by high density forest while the west and the south-western parts are characterized by sparser vegetation and agricultural fields.

AVAILABLE DATA

The data sets used in this study are of different types: satellite data are in digital raster format while the rainfall data are point data. The available images are a set of NOAA-AVHRR scenes, acquired between January 1988 and May 2005, with one month frequency (209 images). These images have been made public by the *National Environmental Satellite, Data and Information Service* (NESDIS) (www.class.noaa.gov) in the level b format. The images have been recorded by different platforms (from NOAA-9 to NOAA-17).

Monthly rainfall data records for 1988–2000 from 247 stations across Sicily, from the *Ufficio Idrografico Regionale* (UIR) data set, have been used to derive a time series of monthly precipitation.

METHODS

Data were processed by two different techniques: a chain of image processing for remotely sensed data and a method of spatial interpolation (*geographically weighted regression with a residual kriging*) for the rainfall (Bono *et al.*, 2005). These techniques were used to create a complete data set for the study period. Time series analysis both on the images and rainfall data sets was also performed.

SATELLITE DATA PRE-PROCESSING

All satellite imagery were geocorrected (datum UTM European 1950), then a chain of calibration processes was implemented. Radiances for the first two channels (red and NIR) were calibrated first. In this step, different equations for each sensor were applied in order to account for sensor degradation. For NOAA 9, 11 and 12 the following equation was applied (Che & Price, 1992):

$$L_\lambda = \alpha\, e^{\beta\,(d-\varepsilon)} \cdot (C_{10} - \varphi) \tag{2}$$

where L_λ is the radiance value, α, β, ε and φ are calibration parameters related to wavelength, C_{10} is the raw 10 bit Digital Number (DN) and d is the aging factor. For NOAA 10, 14, 16 and 17, the following equation was applied (Nagaraja Rao, 2001):

$$L_\lambda = \alpha\,(C_{10} - \beta) \tag{3}$$

After the in-radiance calibration, the reflectance values were calculated by the application of the Epema formula (Epema, 1990) and, subsequently, the whole data set was corrected from the atmospheric influence by the application of the relative scattering method (Chavez *et al.*, 1988).

In order to obtain an accurate descriptor of the vegetation coverage density, the spatial distribution of the well known fractional cover *Fr* (Carlson & Ripley, 1997), has been computed for each month. The *Fr* values have been obtained by the application of the following equation:

$$Fr = \left[\frac{NDVI - NDVI_{min}}{NDVI_{max} - NDVI_{min}} \right]^2 \qquad (4)$$

where $NDVI_{min}$ and $NDVI_{max}$ are the minimum and the maximum values found in the whole data set, respectively, excluding the *NDVI* negative and zero values.

TIME SERIES ANALYSIS

A PCA on the NDVI data set has been applied in order to identify the patterns and the physical processes embedded in the observed variable by means of the analysis of few principal components (PC_s).

In order to detect vegetation index trends, anomalies, evolution and its relationship between the rainfall spatial and temporal distribution, a TSA both on standardized and non standardized values of NDVI and rainfall has been carried out. The variables standardization was applied in order to remove the normal seasonal oscillations from both data sets. In this way it is possible to perform a trend and anomalies detection analysis for the period under investigation.

In order to standardize the data set, the following expression has been applied:

$$Z(i,j) = \frac{X(i,j) - \mu(i)}{\sigma(i)} \qquad (5)$$

where i and j are the month and year, respectively, $Z(i, j)$ is a generic pixel value of an image of NDVI or monthly rainfall P, $\mu(i)$ and $\sigma(i)$ are the mean and standard deviation, respectively, calculated for the month i, for the considered pixel values, over the period under investigation. The standardized data set has been used in order to detect trends, anomalies and correlations, while on the other hand, the non-standardized data set has been used for the correlation analysis between NDVI and rainfall data sets.

In order to consider homogeneous areas of the region, a subdivision using the mean vegetation amount and the mean precipitation criteria was performed. The fractional cover monthly data set was used to calculate the mean fractional cover spatial distribution, Fr_m that can be easily used to identify the main vegetation density classes over the period under investigation. The vegetation classes (sub-zones) have been defined by the examination of the Fr_m image histogram and by the knowledge of the main characteristics of the vegetation existing over the territory under analysis. The TSA has been carried out on the whole Sicily region, and then has been repeated on Fr_m and of mean annual precipitation (MAP) sub-zones over the period, as reported in Table 1.

Table 1 Summary of the range selected both for the Fr_m and mean annual precipitation.

Mean fractional cover (Fr_m) (–)			Mean annual precipitation (MAP) (mm)		
low range	medium range	high range	low range	medium range	high range
0–0.3	0.3–0.6	0.6–1	<600	600–850	>850

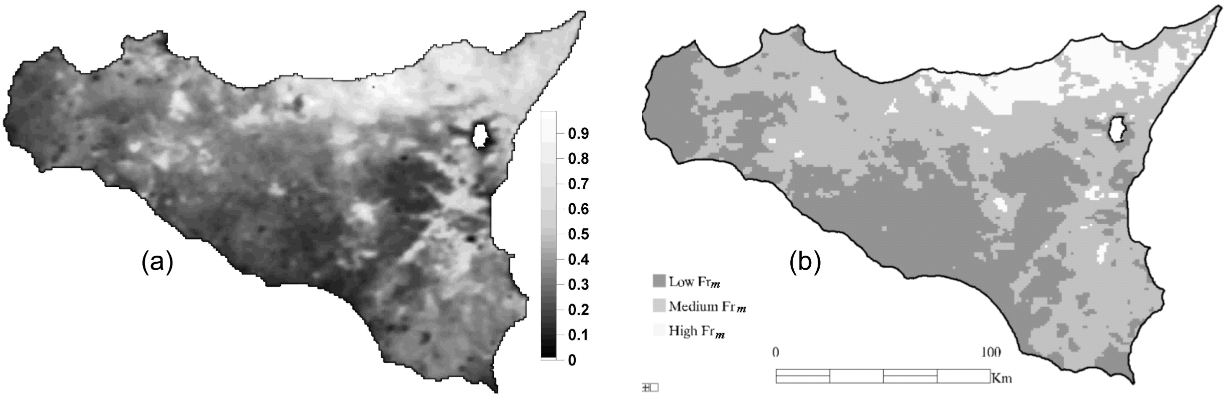

Fig. 2 Mean fractional cover distribution (a) and subdivision in classes of vegetation density (b).

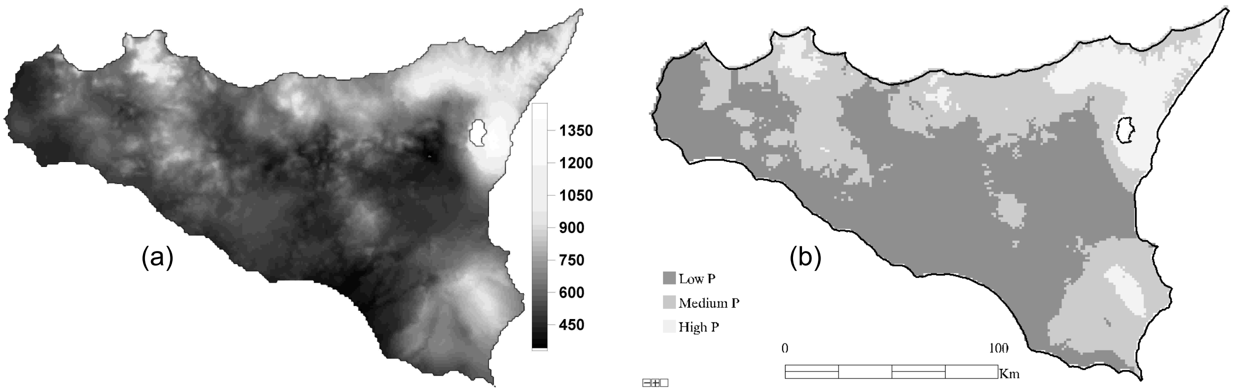

Fig. 3 Mean annual rainfall distribution (a) and its subdivision in classes (b).

The subdivisions are illustrated in Figs 2 and 3. The NDVI-precipitation relationship at a regional scale has been demonstrated with a cross-correlation analysis. The cross-correlation is a measure of similarity of two signals, commonly used to find features in an unknown signal by comparing it to a known one. It is a function of the relative time between the signals and it is based on the cross-correlogram that is the graph of the cross-correlation coefficients versus the time lags l.

The time series of monthly precipitation and NDVI have been analysed using the Mann-Kendall non-parametric test for trend. Mann (1945) originally used this test and Kendall (1962) subsequently derived the test statistic distribution. This test allows inquiries on the presence of a tendency of long period in rainfall data, without having to make an assumption about its distributional properties. Moreover the non parametric methods are less influenced by the presence of outliers in the data compared with other methods.

In trend test the null hypothesis H_0 is that there is no trend in the population from which the data set is drawn; hypothesis H_1 is that there is a trend in the analysed records. Mann-Kendall test was applied to monthly data set. The test statistic, Kendall's S, (Kendall, 1962) is calculated as:

$$S = \sum_{i=1}^{n-1} \sum_{j=i+1}^{n} sign(y_j - y_i) \tag{6}$$

where y are the data values at times i and j, n is the length of the data set and:

$$sign(\vartheta) = \begin{cases} 1 & if\ \vartheta > 0 \\ 0 & if\ \vartheta = 0 \\ -1 & if\ \vartheta < 0 \end{cases} \tag{7}$$

The Mann-Kendall test has two parameters that are of importance for trend detection. These parameters are the significance level that indicates the test strength, and the slope magnitude estimate that indicates the direction as well as the magnitude of the trend. Under the null hypothesis that y_i are independent and randomly ordered, the statistic S is approximately normally distributed when $n \geq 8$, with zero mean and variance as follows:

$$\sigma^2 = \frac{n(n-1)(2n+5)}{18} \tag{8}$$

The standardized test statistic Z, computed by:

$$Z = \begin{cases} \frac{S-1}{\sigma} & if\ S > 0 \\ 0 & if\ S = 0 \\ \frac{S+1}{\sigma} & if\ S < 0 \end{cases} \tag{9}$$

follows a standard normal distribution (Kendall, 1962). In this analysis confidence levels at 90, 95 and 99 percent were considered. The non-parametric robust estimate of the magnitude of the slope, β, of linear trend, determined by Hirsch *et al.*, (1982), is given by:

$$\beta = Median\left[\frac{(y_j - y_i)}{(j-i)}\right] \tag{10}$$

RESULTS

In disagreement with previous literature (Gurgel & Ferreira, 2003), in our case the first principal component (I PC) explains only a percentage of 47% of the total variance of the data set and each other components explain a significant percentage of the total variance. This result will be investigated in a more detailed way in a future research.

However, the first principal component negative and positive values distribution (Fig. 4(a)) clearly separates the zones characterized by monthly mean NDVI values

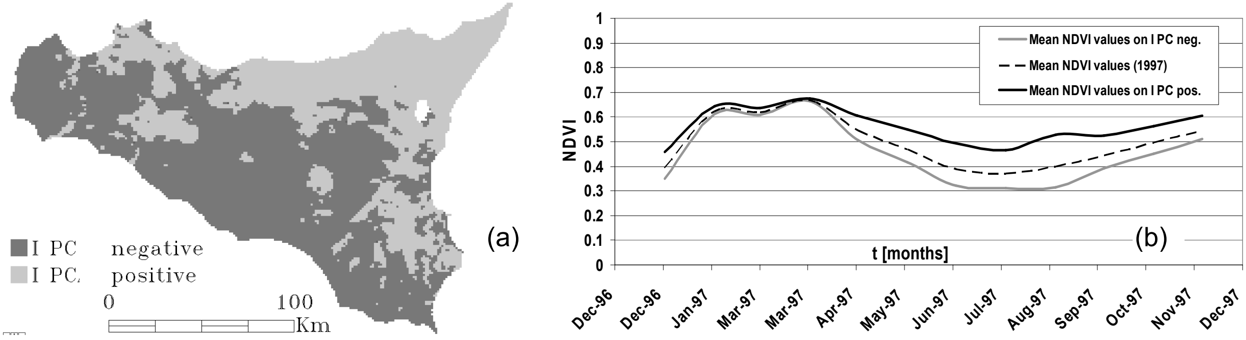

Fig. 4 Positive and negative value zones of I PC (a) and monthly mean NDVI values for each zone compared to the regional ones (b).

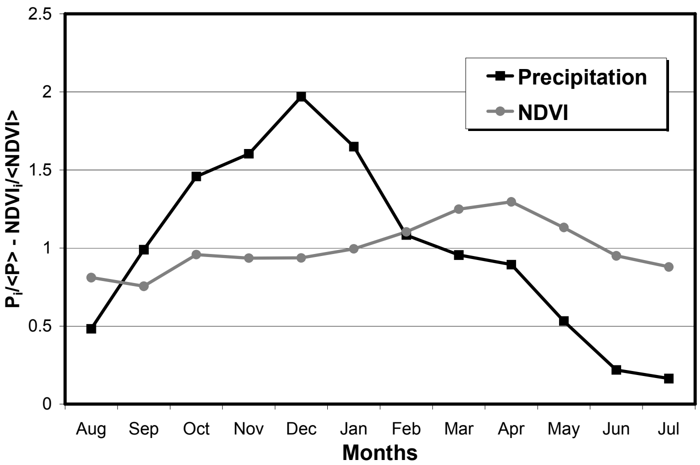

Fig. 5 Time lag between NDVI and precipitation (normalized by the annual mean).

above the regional mean (positive I PC values) from the ones characterized by NDVI monthly mean values below the regional mean (negative I PC values): this behaviour has been found for each year of the data set. Figure 4(b) shows the situation for 1997.

The normalized seasonal cycle (seasonal cycle divided by the annual mean) of NDVI and precipitation, shown in Fig. 5, points out a time lag between the two variables equal to four months (December for precipitation and April for NDVI).

Similar information can be obtained from the analysis of the cross-correlogram between NDVI and precipitation time series for the Sicily as whole, for the three zones of fractional cover (high Fr_m, medium Fr_m and low Fr_m) and for the three zones of mean annual precipitation (high MAP, medium MAP and low MAP). The analysis of cross-correlogram (Fig. 6) points out that current vegetation is affected by antecedent precipitation of the past few months.

It is observed that correlations change with lag and are positive at lags 6–8 months in most cases. Higher correlations tend to occur between 4 and 6 month lags. Also, the correlation-lag pattern, especially the peak-lag (lag with the highest correlation), varies depending on the fractional cover class Fr_m used and MAP.

The maximum correlation between NDVI and precipitation occurs at a time lag equal to 4 months for all the examined cases, except for high Fr_m and high MAP cases

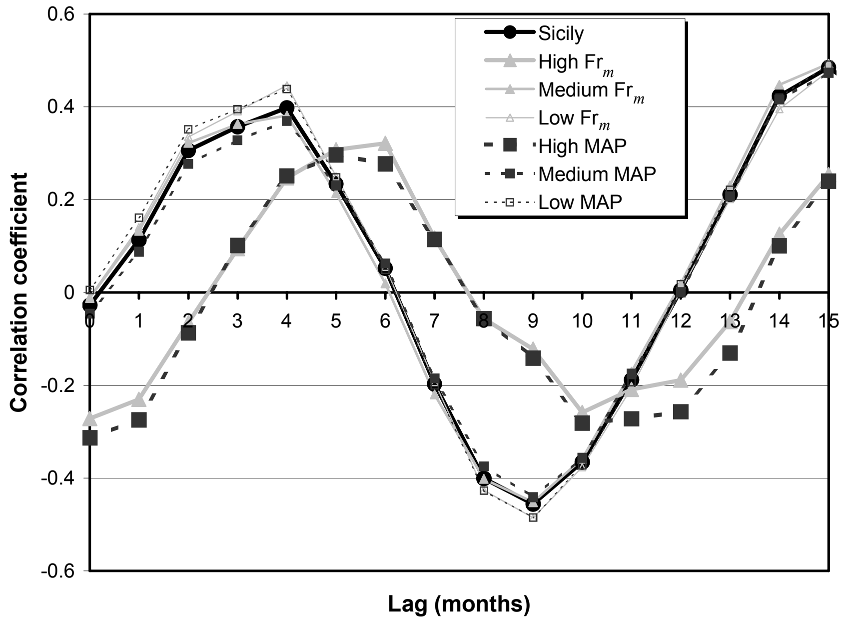

Fig. 6 Cross-correlogram between precipitation and NDVI.

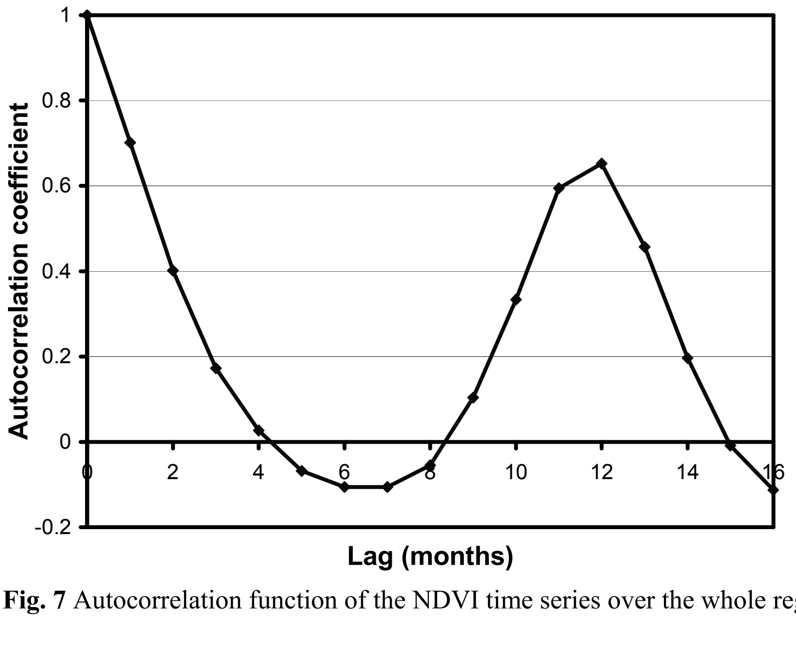

Fig. 7 Autocorrelation function of the NDVI time series over the whole region.

(equal to 6 months). The peak of cross-correlogram indicates that the maximum influence of precipitation on vegetation index occurs in the fourth month for Sicily as a whole, and for the areas characterized by low-medium fractional cover or by low-medium MAP.

The areas characterized by high fractional cover or high MAP (i.e. the forested areas) show a lag time between precipitation and NDVI greater then the other areas and equal to five months (high MAP) or six months (high Fr_m). This could be due to the slow response of wooded areas.

A similar analysis has been carried out on the cumulative rainfall to relate the vegetation distribution of a generic month to the total rainfall of 2, 3, 4, 5 and 6 months before. Results give similar indications reported above, enforcing the idea that the strongest influence on the vegetation is mainly due to precipitation that occurred 4 months before. Moreover, considering that the mean NDVI peak occurs generally on April, it seems to be reasonable that the mean rainfall value of December affects this peak value.

The vigour of the current vegetation is highly affected by antecedent vegetation vigour of the past few months. The changes in vegetation vigour have a low-frequency pattern compared with atmospheric phenomena. This was confirmed by autocorrelation analysis of the NDVI time series. A positive autocorrelation was detected at lag times of up 2 months, but decreased with increasing lag length. Correlation coefficients are usually greater than 0.7 at a lag of 1 month and then decrease to 0.4 at lags of 2 months (Fig. 7).

Trend analysis on precipitation and NDVI

Table 1 shows the results of a Mann-Kendall test on the different time series used in the study. The trend analysis was carried out using a continuous series of original (not standardized, *NS*) monthly precipitation and NDVI (Fig. 8).

Table 1 Mann-Kendall non-parametric test for trend results (*NS* = not standardized; *S* = standardized).

Variables		Significance level			Trend coefficient
		$\alpha = 0.1$	$\alpha = 0.05$	$\alpha = 0.01$	
P (*NS*)		No Trend	No Trend	No Trend	–
NDVI (*NS*)		Trend	Trend	Trend	–0.000829
P (*NS*)	Low Fr_m	No Trend	No Trend	No Trend	–
	Medium Fr_m	No Trend	No Trend	No Trend	–
	High Fr_m	No Trend	No Trend	No Trend	–
NDVI (*NS*)	Low Fr_m	Trend	Trend	Trend	–0.001007
	Medium Fr_m	Trend	Trend	Trend	–0.000768
	High Fr_m	No Trend	No Trend	No Trend	–
P (*NS*)	Low Fr_m	No Trend	No Trend	No Trend	–
	Medium Fr_m	No Trend	No Trend	No Trend	–
	High Fr_m	No Trend	No Trend	No Trend	–
NDVI (*NS*)	Low Fr_m	Trend	Trend	Trend	–0.000903
	Medium Fr_m	Trend	Trend	Trend	–0.000842
	High Fr_m	Trend	Trend	No Trend	–0.000620
P (*S*)		No Trend	No Trend	No Trend	–
NDVI (*S*)		Trend	Trend	Trend	–0.006288
P (*S*)	Low Fr_m	No Trend	No Trend	No Trend	–
	Medium Fr_m	No Trend	No Trend	No Trend	–
	High Fr_m	No Trend	No Trend	No Trend	–
NDVI (*S*)	Low Fr_m	Trend	Trend	Trend	–0.004365
	Medium Fr_m	Trend	Trend	Trend	–0.003943
	High Fr_m	Trend	Trend	No Trend	–0.002793

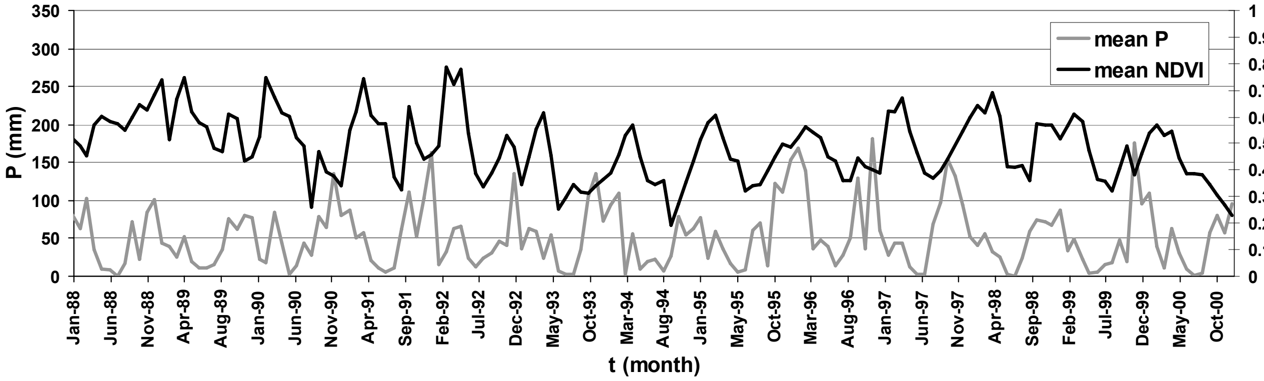

Fig. 8 Non-standardized monthly precipitation and NDVI.

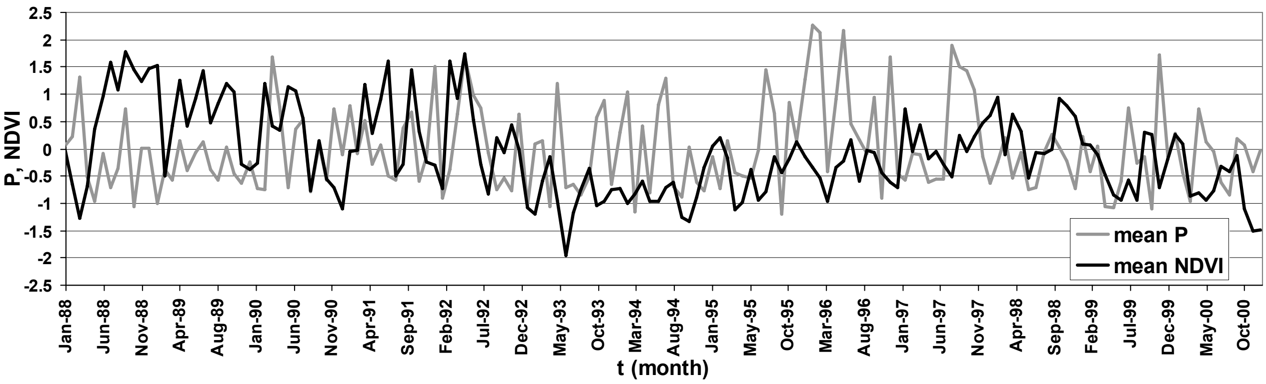

Fig. 9 Standardized monthly precipitation and NDVI.

The presence of a regional trend for NDVI is confirmed until the 99% confidence level, while there is no trend for precipitation at any significance level. Similar results can be obtained using the not standardized NDVI and precipitation for the three zones of fractional cover and for the three zones of mean annual precipitation: any trend is absent for precipitation, while NDVI shows a negative trend at any significance level for low-medium Fr_m and for low-medium MAP and the absence of any trend for high Fr_m, indicating a substantial stability of dense vegetation in the considered period.

In order to remove any influence of seasonality on the analysed time series, a trend analysis on standardized NDVI and precipitation has been carried out (Fig. 9). The results of this analysis confirm the results of the previous one: absence of trend for precipitation, and presence of a statistically significant trend for NDVI, especially in areas characterized by low and medium fractional cover. However, the estimated trend coefficients are weak, confirming a substantial stability of the vegetation in Sicily.

The different trends behaviour between vegetation and rainfall could be explained by the fact that, in order to describe vegetation dynamics, the use of precipitation alone is insufficient, and other parameters, such as temperature oscillations, have to be considered in the analysis as found by other authors (Schultz & Halpert 1993; Wang *et al.*, 2001).

CONCLUDING REMARKS

The aim of this work was to investigate the vegetation response to rainfall variation in Sicily during the 1988–2000 period, by means of rainfall and NDVI time series analysis. In particular, the NDVI distributions have been derived by the processing of NOAA-AVHRR satellite images.

The analysis of the mean NDVI trend has been carried out in the whole region and in three sub-zones characterized by low, medium and high mean vegetation fractional cover. The trends analysis showed a weak decreasing of vegetation coverage despite an absence of trends in rainfall mean distribution.

The cross-correlation function showed a lag time variable from 4 to 6 months between the mean NDVI and precipitation signals, depending on the vegetation fractional cover class and on the MAP class.

Some issues still remain to be investigated:

– the influence of air temperature variation on NDVI evolution: i.e. the use of a synthetic climate index, like the Thornthwaite aridity index or the evaporative fraction, could give the combined influences of both temperature and precipitation;
– different vegetation types have different response due the phenological cycle: for this reason, a similar analysis on different vegetation types needs to be carried out;
– the use of a distance-based vegetation index could be appropriate in order to avoid the well know soil influence on the NDVI vegetation index and the NDVI saturation problems in biomass quantification.

All these topics could be dealt with by also using the recent years data set. In conclusion, TSA analysis of satellite-derived vegetation indices and climatic data has been proven to be a powerful tool to analyse large amounts of data and to produce understandable results.

Acknowledgements Special thanks are due to Salvatore Nizza and Antonino La Motta for their helpful collaboration in satellite image pre-processing.

REFERENCES

Aber, J. S., Wallace, J. & Nowak, M. C. (2002) Response of forest to climatic events and human management at Fort Leavenworth, Kansas. Kansas Geological Survey, *Current Res. Earth Sci. Bull.* **248**(1). Available at http://www.kgs.ukans.edu/Current/2002/aber/aber1.html.

Bono, E., La Loggia, G. & Noto, L. V. (2005) Spatial interpolation methods based on the use of elevation data. *Geophys. Res. Abstracts* **7**, 08893, EGU 2005.

Carlson, T. N. & Ripley, D. A. (1997) On the relation between NDVI, fractional vegetation cover, and leaf area index. *Remote Sens. Environ.* **62**, 241–252.

Chavez, P. S. (1988), An improved dark-object subtraction technique for atmospheric scattering correction of multispectral data. *Remote Sens. Environ.* **24**, 459–479.

Che, C. L. & Price, J. C. (1992) Survey of radiometric calibration results and methods for visible and near-infrared channels of NOAA-7,-9, and -11 AVHRR. *Remote Sens. Environ.* **41**, 19–27.

Cuomo, V., Lanfredi, R., Lasaponara, M. F., Macchiato, M. F. & Simoniello, T. (2001) Detection of interannual variation of vegetation in middle and southern Italy during 1985–1999 with 1 km NOAA AVHRR. *J. Geophys. Res.* **106**(D16), 17 863–17 876.

Epema, G. F. (1990) Determination of planetary reflectance for Landsat 5 Thematic Mapper tapes processed by Earthnet (Italy). *Esa J.* **14**, 101–108.

Geeson N. A., Thornes J. B. & Brandt C. J., (2002) *Mediterranean Desertification: A Mosaic of Processes and Responses*, Wiley & Sons, Chichester, UK.

Gurgel, H. C. & Ferreira N. J. (2003) Annual and interannual variability of NDVI in Brazil and its connections with climate. *Int. J. Remote Sens.* **24**(18), 3595–3609.

Hirsch, R. M., Slack, J. R. & Smith, R. A. (1982) Techniques of trend analysis for monthly water quality data. *Water Resour. Res.* **18**, 107–121.

Kendall, M. G. (1962) *Rank Correlation Methods*, 3rd edn. Hafner Publishing Company, New York, USA.

Kosmas C., Ferrara A., Briasouli H. & Imeson A. (1999) Methodology for mapping Environmentally Sensitive Areas (ESAs) to Desertification. In: *The Medalus Project Mediterranean Desertification and Land Use. Manual on Key Indicators of Desertification and Mapping Environmentally Sensitive Areas to Desertification* (ed. by: C. Kosmas, M. Kirkby & N. Geeson), 31–47. European Union 18882. ISBN 92-828-6349-2.

Mann, H. B. (1945) Non parametric tests again trend. *Econometrica* **13**, 245–259.

Martiny, N., Camberlin, P., Richard, Y. & Phillippon, N. (2006) Compared regimes of NDVI and rainfall in semi-arid regions of Africa. *Int. J. Remote Sens.* **27**(23–24), 5201–5223.

Nagaraja Rao, C. R. (2001) Implementation of the post-launch vicarious calibration of the GOES imager visible channel. *NOAA/NESDIS Office of Research and Applications Camp Springs, (May 4, 2001), Maryland 20746, USA*.

Potter, C. S. & Brooks, V. (1998) Global analysis of empirical relations between annual climate and seasonality of NDVI. *Int. J. Remote Sens.* **19**, 2921–2948.

Richard, Y. & Poccard, I. A. (1998) A statistical study of NDVI sensitivity to seasonal and interannual rainfall variation in Southern Africa. *Int. J. Remote Sens.* **19**, 2907–2920.

Rouse, J. W. Jr., Haas, R. H., Deering, D. W., Schell, J. A. & Harlan, J. C. (1974) Monitoring the vernal advancement and retrogradation (green wave effect) of natural vegetation. *NASA/GSFC Type III Final Report, Greenbelt, Maryland, USA.*

Saugier, B. (1996) *Végétation et atmosphere.* Dominos Flammarion, France.

Schultz, P. A. & Halpert, M. S. (1993) Global correlation of temperature, NDVI and precipitation. *Adv. Space Res.* **13**, 277–280.

Wang, J., Price, K. P. & Rich, P. M. (2001) Spatial patterns of NDVI in response to precipitation and temperature in the central Great Plains. *Int. J. Remote Sens.* **22**, 3827–3844.

Woldu Tamrat, J. (1997) Remote sensing of biomass production, radiation distributions, and rainfall patterns. Senior Thesis Report. Physics Department, University of Asmara. Advisor: Robert Van Buskirk, Department of Energy.

Zhang, X., Friedl, M. A., Schaaf, C. B., Strahler, A. H. & Liu, Z. (2005) Monitoring the response of vegetation phenology to precipitation in Africa by coupling MODIS and TRMM instruments *J. Geophys. Res*. **110**, D12103, doi:10.1029/2004JD005263.